An Additional Methyl Group at the 10-Position of Retinal Dramatically Slows down the Kinetics of the Rhodopsin Photocascade†

Frank DeLange,‡ Petra H. M. Bovee-Geurts,‡ Jenny VanOostrum,‡ M. Daniël Portier,‡ Peter J. E. Verdegem,§ Johan Lugtenburg,§ and Willem J. DeGrip*,‡

Department of Biochemistry FMW-160, Institute of Cellular Signalling, University of Nijmegen, P.O. Box 9101, 6500 HB Nijmegen, The Netherlands, and Leiden Institute of Chemistry, Gorlaeus Laboratories, University of Leiden, 2300 RA Leiden, The Netherlands

Received September 26, 1997; Revised Manuscript Received November 17, 1997

ABSTRACT: The present study focuses on ligand−protein interactions in a rhodopsin analogue generated from bovine opsin and the 10-methyl homologue of 11-*cis*-retinal. The analogue pigment displays a reduced α-band at 506 ± 2 and a stronger *β*-band at 325 nm. Remarkably, the rotational strength of these bands observed in visible circular dichroism spectra was found to be similar for both native and 10-methyl rhodopsin. The quantum yield of the analogue pigment was determined to be 0.55. All photointermediates were analyzed by Fourier transform infrared difference spectroscopy. At the batho stage, strong hydrogen-out-of-plane vibrations were observed, indicating that the 10-methyl chromophore also adopts a distorted all-trans conformation at this stage. In contrast to native rhodopsin, the batho intermediate of the 10-methyl pigment is stable up to 180 K and only slowly decays to the next intermediate between 180 and 210 K. As in native rhodopsin, the 10-methyl metarhodopsin I intermediate is generated at about 220 K, but its transition to the metarhodopsin II state is again shifted to a much higher temperature (>293 K) than for the native pigment (>260 K). Infrared analysis, nevertheless, shows that the conformational changes in the photointermediates of the 10-methyl pigment are basically identical with those observed in the native pigment. This is supported by a signal function assay, showing that the analogue pigment is able to activate transducin. The dual effect of the 10-methyl group on the photocascade is attributed to steric interactions which, initially, hamper the relaxation of strain in the polyene chain of the chromophore and, eventually, interfere with the conformational rearrangements of the protein moiety required to adopt the active conformation of the receptor. Our data provide direct support for the concept that the relaxation of strain in the retinal polyene chain acts as the major driving force of the photocascade dark reaction.

Rhodopsin is the photosensor in the vertebrate retinal rod cell and consists of the protein opsin and a photosensitive group (11-*cis*-retinal), linked via a protonated Schiff base to Lys296 of opsin. Photoexcitation of rhodopsin initiates a series of at least four discrete, structurally and spectrally distinct, intermediates. The light-dependent reaction, isomerization of the retinal group to the all-*trans*-conformation, generates the first well-characterized photoproduct: bathorhodopsin. The subsequent dark reaction (batho- to lumirhodopsin and subsequently to metarhodopsin I and II) involves conformational rearrangements in both chromophore and protein. This entire process, called photocascade, culminates within milliseconds after illumination in the active conformation, metarhodopsin II (MetaII),[1] which binds and activates the G-protein transducin (*1, 2*). To date, the most detailed structural information on the photocascade of rhodopsin has been obtained by resonance Raman (RR) and Fourier transform infrared (FTIR) spectroscopy. FTIR difference spectroscopy of the various transitions proved to be extremely powerful since it monitors structural changes in both chromophore and protein which are accompanied by shifts in vibrational frequency, bandwidth, or band intensity. Site-directed mutagenesis and isotope labeling allowed identification of some of the difference bands in these spectra (*3*−*5*). In this way, it was shown that the majority of peaks in the rhodopsin to Batho difference spectra derive from the chromophore, while the subsequent transitions present a gradual increase in protein activity (*6, 7*). The intense hydrogen-out-of-plane (HOOP) vibrations in the rhodopsin to Batho FTIR difference spectra are correlated with those observed in RR spectra of bathorhodopsin and are regarded to reflect twisting around the single bonds in

† This work was supported by grants from The Netherlands Organization for Scientific Research, Subdivision for Chemical Research (NWO-SON, WGM 330-011) and the Space Research Organization of The Netherlands (SRON, MG-031) to W.J.D. and the European Community Biotechnology Program CEC (Project PL 92-0467) to P.J.E.V. and J.L.

* Address correspondence to this author. Fax: +31-243540525. Phone: +31-243614263. E-mail: wdegrip@baserv.uci.kun.nl.

‡ University of Nijmegen.

§ University of Leiden.

[1] Abbreviations: 10-Me-rhodopsin, opsin regenerated with 11-*cis*-10-methylretinal; Batho, bathorhodopsin; DoM, dodecylmaltoside; FTIR, Fourier transform infrared; Lumi, lumirhodopsin; MetaI, metharhodopsin I; MetaII, metarhodopsin II; RR, resonance Raman spectroscopy.

S0006-2960(97)02397-0 CCC: $15.00
Published on Web 02/03/1998

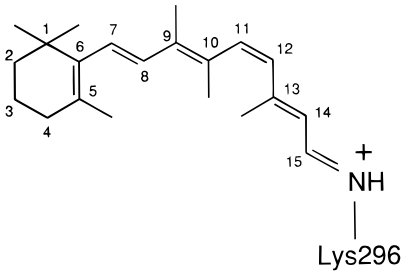

FIGURE 1: Schematic representation of 11-*cis*-10-methylretinal attached to Lys296 of opsin.

the chromophore induced by steric ligand−protein interactions (*8*−*10*). Torsional strain in the chromophore and charge separation between the Schiff base and its counterion have been proposed as potential mechanisms to store the photon energy in the rhodopsin to bathorhodopsin transition (*11*−*13*). Recent work has shown that out-of-plane distortions in the retinal polyene chain, apart from being a highly efficient means of energy storage at the Batho stage, also may contribute to the ultrafast isomerization kinetics in rhodopsin (*14*, *15*). Moreover, since both RR and NMR data show that the environment of the Schiff base does not change significantly in the transition from rhodopsin to bathorhodopsin (*16*, *17*), the concept that the photon energy is stored as torsional strain in the retinal polyene chain is gradually gaining support. The picture emerges that, at the Batho stage, close contacts occur between the isomerized ligand and opsin which hold the former in a strained conformation and function as "contact points" by which the torsional strain in the polyene chain is mediated to drive the conformational changes in the protein moiety.

Potential candidates to mediate steric interactions between opsin and retinal are the protruding retinal side-chain methyl groups. Single demethyl analogs of rhodopsin (9-demethyl and 13-demethyl) have been examined before and show distinct effects on rhodopsin functionality (see, for recent reviews, refs 18 and 19). We have taken the alternative approach and are in the process of evaluating the effects of single methyl group additions. We have started to analyze one of the most critical positions: C_{10} (Figure 1). Although the 10-methyl homolog of 11-*cis*-retinal has earlier been shown to produce a pigment (*20*), effects of the additional methyl group on the photocascade have never been reported. The data presented here show that the extra methyl group has a 2-fold effect on rhodopsin's photocascade: firstly, it stabilizes the strained conformation of the all-*trans*-chromophore up to 210 K and, secondly, it interferes with the conformational rearrangements in the receptor necessary to adopt the active conformation (MetaII), which binds and activates transducin. These results emphasize the importance of finely tuned ligand−protein interactions to guide the photocascade of rhodopsin.

MATERIALS AND METHODS

Synthesis of 11-cis-10-methylretinal. The synthesis of 10-methylretinal was accomplished by a Horner-Wadsworth-Emmonds (HWE) coupling of 2-(diethylphosphono)propionitrile, prepared from proprionitrile and diethylchlorophosphate, with β-ionone. After dibal reduction of the nitrile to an aldehyde function, the conjugated chain was elongated by a HWE coupling of 4-(diethylphosphono)-3-methyl-2-butene nitrile and subsequent dibal reduction to form the aldehyde. The all-*E* isomer of 10-methylretinal was purified using silicagel column chromatography (eluent 20% ether/petroleumether). Overnight irradiation (at 294 K) in dry acetonitrile using a 100 W tungsten incandescent lamp resulted in a photostationary mixture of geometric isomers. Two subsequent HPLC runs, performed as described (*20*), yielded a fraction containing at least 95% 11-*cis*-10-methylretinal, which was used for generation of the analogue pigment. The purity of the compounds was verified using ^{1}H and ^{13}C NMR and mass spectrometry.

Table 1: Efficiency of Extraction of Excess Retinal Oxime from Rhodopsin Membranes Using Bovine Serum Albumin (BSA) or β-Cyclodextrin[a]

	extraction		
		β-cyclodextrin	
membrane pellet	bovine serum albumin [4% (w/v)]	5 mM	10 mM
rhodopsin recovered (%)	83	92	89
A_{280}/A_{500}	3.7	2.5	2.4
oxime remaining[b] (%)	16[c]	52[c]	26[c]

[a] A 2-fold molar excess of retinal was added to a membrane suspension of ROS (buffer A, 4 °C), and converted into oxime by addition of hydroxylamine, resulting in an initial A_{280}/A_{500} ratio of 2.6. After 1 h extraction the membranes were pelleted, washed with buffer A and their A_{280}/A_{500}, rhodopsin content and oxime content was determined after solubilization in 20 mM nonylglucose in buffer A. Repeated extraction with BSA or 10 mM cyclodextrin only slightly further reduces the percentage oxime left. [b] Calculated from A_{365}/A_{500}. [c] Variance in these numbers is 20%.

Generation of 10-methyl rhodopsin. Bovine rod outer segments in the opsin form (opsin membranes) were prepared from fresh, light-adapted, eyes as described (*21*). The regeneration capacity of these preparations was estimated from the A_{500}/A_{280} ratio obtained upon subsequent incubation with a 3-fold excess of 11-*cis*-retinal, whereby a ratio of 2.0 was taken to represent membranes with maximal rhodopsin content. Rhodopsin and 10-Me-rhodopsin were prepared from opsin membranes showing a regeneration capacity in the range 90−100%. All manipulations were done under dim red light (>620 nm, Schott RG620 cutoff filter).

Analogue pigments were generated by incubating opsin membranes with a 3-fold molar excess of 11-*cis*-10-methylretinal at room temperature. Opsin membranes were suspended in buffer A (20 mM Pipes, 130 mM NaCl, 5 mM KCl, 2 mM $CaCl_2$, 0.1 mM EDTA, and 1 mM dithioerythreitol, pH 6.5), to a final concentration in opsin of 100 μM. The retinals were added in a small volume of dimethylformamide (≤2% final volume) and the incubation was performed in an inert atmosphere (nitrogen or argon). Excess retinal was then converted into the oxime by addition of hydroxylamine to a final concentration of 10 mM. To remove the large excess of oxime, a novel procedure was developed. Extraction with 10 mM solutions of heptakis (2,6-di-O-methyl)-β-cyclodextrin (Aldrich), which produces a soluble inclusion complex with retinals and retinaloximes, removes 70−80% of the excess retinoid. This procedure is almost as efficient as extraction by high concentrations of bovine serum albumin (Table 1). However, it does not leave a difficult to remove protein residue nor does it affect the functionality of rhodopsin (J. VanOostrum and W. J. DeGrip, unpublished material). To further reduce residual oxime, higher cyclodextrin concentrations were employed, but this

also leads to partial lipid extraction. Three extractions with 50 mM β-cyclodextrin in buffer A (4 °C) followed by washing twice with doubly distilled water removed over 95% of the excess retinal according to HPLC analysis (*22*). To restore the native lipid/protein ratio, the resulting pigments were then dissolved in 20 mM nonylglucose in buffer A and mixed with a 50-fold molar excess of retina lipids isolated as described (*23*). Reconstitution in proteoliposomes was accomplished by stepwise dilution (*24*). The resulting proteoliposomes were finally washed with doubly distilled water and stored at −80 °C until further use.

Spectral Properties of the 10-Methyl Pigment. UV−visible spectra of proteoliposomes suspended in buffer A (either Mes, Pipes, or Bis-Tris propane, pH as indicated) to a final concentration of 1 μM in pigment were recorded on a Perkin-Elmer λ 15 double beam spectrometer equipped with an end-on photomultiplier detector. A circulating bath was used to control sample temperature. The sample was bleached with yellow light (Schott OG530 cutoff filter). The wavelength of maximal absorbance (λ_{max}) of rhodopsin and the 10-Me analogue was determined from the peak position in the difference spectrum obtained by subtracting the spectrum after illumination from the dark state spectrum, both taken in the presence of 10 mM hydroxylamine in mixed micellar solution (20 mM DoM in buffer A). The metarhodopsin I−metarhodopsin II equilibrium was studied in proteoliposomes as described for rhodopsin (*25*).

Circular Dichroism. UV−visible circular dichroism spectra were recorded for solubilized pigment samples (40 mM DoM in buffer A, 10 °C) in order to compare the overall conformation of the 10-methyl chromophore with that of the native chromophore in the binding pocket of opsin. Solutions, containing about 22 μM pigment, were analyzed on a Jasco J-715 spectropolarimeter. Calibration of the instrument was checked before and after the measurements using a 0.06% (w/v) aqueous solution of d-10-camphor sulfonate.

Photosensitivity of the 10-Methyl Pigment. The quantum yield of 10-Me-rhodopsin was determined relative to that of rhodopsin (*26*−*28*). The quantum yield ($\Phi_{Rh} = 0.67$) and extinction coefficient at λ_{max} ($\epsilon_{Rh} = 40.600 \pm 500$ M^{-1} cm^{-1}) of rhodopsin are both well characterized experimentally (*26*). Rhodopsin and 10-Me-rhodopsin were solubilized in buffer A (Pipes, pH 6.5) with 10 mM DoM and 10 mM hydroxylamine to give an absorbance at 497 nm of 0.16 ± 0.007 OD/cm. Solutions were kept at 10 °C and illuminated under low-bleaching conditions through a 497 ± 5 nm interference filter. The illumination conditions were such that the half-time of pigment bleaching was between 30 and 60 min. Spectra were taken as function of illumination time until the absorbance at 497 nm was below 3% of its initial value. The half-time of pigment (absorbance) decay in the dark, providing a measure of pigment stability under the described experimental conditions, was determined to be >20 h.

A plot of the function $\log [I_t/(I_f - I_t)]$ versus illumination time was shown to yield a straight line of which the slope (S) is a measure of the photosensitivity ($\epsilon\Phi$) of a visual pigment (*26*). Here, I_t is the excitation light transmission as a function of time, and I_f is the transmission after complete bleaching. Since in our experiments absorbance data were collected, we converted the above function to $A_f - \log[10^{A_t} - 10^{A_f}]$. Here, A denotes the absorbance of the sample at the excitation wavelength. The quantum yield of the 10-methyl pigment (Φ_{An}) was calculated from

$$\Phi_{An} = \frac{S_{An}}{S_{Rh}} \frac{\epsilon_{Rh}}{\epsilon_{An}} \Phi_{Rh}$$

As a control, a similar analysis was performed on isorhodopsin (opsin regenerated with 9-*cis*-retinal). For the extinction coefficient of isorhodopsin at λ_{max}, we used $\epsilon_{Iso} = 43.000$ M^{-1} cm^{-1} (*29*). The extinction coefficient of the 10-methyl pigment at the excitation wavelength (497 nm) was determined from separate experiments to be 60 ± 5% of that of rhodopsin (see Results).

FTIR Spectroscopy. FTIR analyses were performed on a Mattson Cygnus 100 spectrometer equipped with a liquid nitrogen cooled, narrow band, HgCdTe detector. Spectra were taken at 4 cm^{-1} resolution unless stated otherwise. Sample temperature was computer controlled using a variable temperature cell (Graseby Specac), which was evacuated and had a set of NaCl windows in the infrared light path. Samples, prepared by isopotential spin-drying 2−3 nmol of pigment on an AgCl window (Fisher Scientific Co.), were rehydrated and sealed using a second AgCl window and a rubber O-ring spacer as described (*3*, *25*, *30*).

Samples were illuminated in the spectrometer using either a 20 W halogen lamp, equipped with a KG1 infrared filter (Schott Mainz, FRG) in combination with a 497 ± 5 nm interference filter, or a modified (150 W halogen) fiberoptics ringilluminator (Schott) equipped with a filterwheel carrying a set of cutoff filters. Typically eight spectra (256 scans each, ∼65 s acquisition time per spectrum) were taken, and averaged, of the dark-state receptor and, subsequently following illumination, of a particular photointermediate state. Difference spectra were calculated by subtracting these blocks of spectra.

To analyze the succesive phototransitions of rhodopsin and the 10-Me analogue, we selected the following illumination scheme. At 90 K, native and analogue samples were illuminated for 40 s with light of 497 nm. The Batho intermediates could be completely photoreversed by illuminating the sample for 130 s with light of ≥610 nm (Schott RG610 cutoff filter), as evidenced from the successive difference spectra. Subsequently, in the case of rhodopsin, the temperature was adjusted to 180 K and by illuminating the sample again with light of 497 nm (40 s) a stable Lumi photointermediate was produced. "Dark state" rhodopsin was recovered from this Lumi sample by cooling to 90 K and subsequent irradiation with red light for at least 3 min (RG610). From here, either the Lumi measurement was repeated or metarhodopsin I was produced by heating to 253 K and irradiation with yellow light (OG530) for 2 min. Metarhodopsin II (OG530, 2 min) was measured at 283 K on a separate sample at 8 cm^{-1} resolution (interferograms were doubly zero-filled prior to further processing yielding an apparent resolution of 4 cm^{-1}). A similar approach was used to collect the analogue pigment data.

Signal Transduction. Transducin activation was monitored using a fluorescence assay as described (*31*, *32*). The enhanced intrinsic fluorescence of activated, i.e., GTP bound, bovine transducin was recorded on a Shimadzu RF-5301PC spectrofluorophotometer (excitation: 295 nm, bandwidth 1.5 nm; emission 337 nm, bandwidth 15 nm). Measurements were carried out at pH 7.4 and 20 °C in a buffer containing

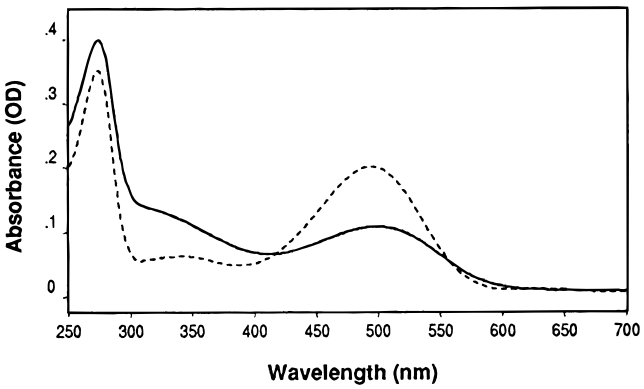

FIGURE 2: UV−visible absorbance spectra of rhodopsin (dashed line) and 10-methyl rhodopsin (solid line). These spectra were taken on the basis of identical amounts of opsin (see text). The difference in absorbance at 280 nm arises from different relative contributions of the β-band at this wavelength.

20 mM HEPPS, 100 mM NaCl, 2 mM $MgCl_2$, 1 mM DTE, and 0.01% (w/v) DoM; the final volume was 2 mL and contained 100 nM transducin and 5 nM of (10-methyl) rhodopsin. A hypotonic extract of isotonically washed rod outer segments served as the source for transducin (*33*). Immediately before data aquisition, the reaction mixture was bleached for 5 min in bright white light. After reaching a steady fluorescence level, GTP-γ-S (Boehringer Mannheim) was added to a final concentration of 2.5 μM and the subsequent increase in tryptophan fluorescence of the α-subunit of transducin ($G_t\alpha$) was monitored.

RESULTS

Pigment Formation. Regeneration of bovine opsin with 11-*cis*-10-methylretinal showed about 6-fold slower kinetics at room temperature than with 11-*cis*-retinal at 15 °C. Nevertheless, the full equivalent of functional opsin produced analogue pigment since the same final amount of analogue pigment was produced with increasing molar excess (3 → 10) of 11-*cis*-10-methylretinal and subsequent incubation with 11-*cis*-retinal did not generate additional rhodopsin. The 10-methyl pigment showed a λ_{max} at 506 ± 2 nm ($n = 5$) as deduced from difference spectroscopy. Figure 2 shows the UV−visible absorbance spectrum of regenerated rhodopsin and the 10-methyl pigment based on identical amounts of opsin. It is obvious that the analogue spectrum has a relatively high β-band, indicative of a distorted chromophore, and that the molar absorbance of the main band is much smaller than that of native rhodopsin. Moreover, by simulating these spectra using three Gaussian band profiles (not shown), the β-band of the 10-methyl pigment was found to be shifted down by 15 nm to 325 nm relative to that of the native pigment. From our data, we estimate the molar extinction coefficient of the analogue at λ_{max} to be 60 ± 5% ($n = 5$) of that of native rhodopsin, i.e., 24.000 ± 2.000 M^{-1} cm^{-1}.

Circular Dichroism. Figure 3 shows the visible circular dichroism (CD) spectra of the native and analogue pigments corrected for the buffer contribution. Less than 1% of the pigments was bleached during the CD experiments. The CD spectrum of rhodopsin is in good agreement with data published previously (*34*−*38*). The rotational strengths of both the α- and β-band of the 10-methyl pigment were found

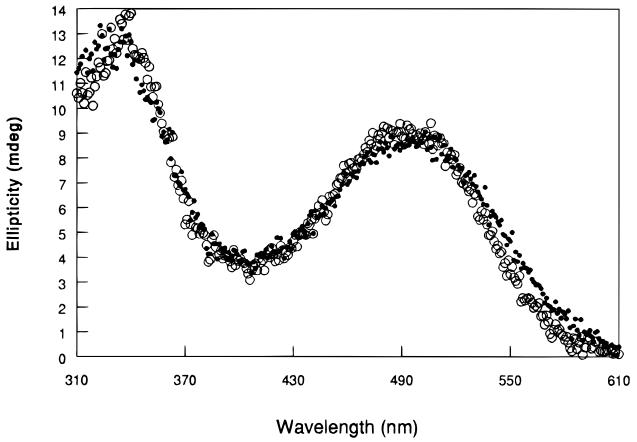

FIGURE 3: Visible circular dichroism spectra of rhodopsin (○) and 10-methyl rhodopsin (●). Ellipticity data are summarized in Table 2. Samples (0.82 OD/cm at λ_{max} for native and 0.55 OD/cm for the 10-methyl pigment) were analyzed in 1 cm path length (quartz) cuvettes, at 10 °C.

Table 2: Relative Circular Dichroism Properties of Native and 10-Methyl Rhodopsin[a]

pigment	$\lambda_{max([\Theta],\alpha)}$	$\lambda_{max([\Theta],\beta)}$	$[\Theta]_{max,\alpha}/A_{max,\alpha}$	$[\Theta]_{max,\beta}/A_{max,\beta}$	$[\Theta]_{max,\beta}/A_{max,\alpha}$
native	490	335	11.0	48.3	15.9
10-Me	500	330	15.4	25.2	21.7

[a] $[\Theta]_{Max(\alpha,\beta)}$ = measured ellipticity at $\lambda_{Max(\alpha,\beta)}$ in mdeg. $A_{max(\alpha,\beta)}$ = measured absorbance at $\lambda_{max(\alpha,\beta)}$ (OD). For discussion of the significance of the $[\Theta]/A$ parameter, see text.

to be essentially similar to those of native rhodopsin. The parameter $[\Theta]_{max}/A_{max}$ relates the maximal ellipticity to the absolute absorbance of a certain band and provides a measure for the conformation of the 10-Me and native chromophore in the binding pocket of opsin (Table 2). Whereas $[\Theta]_{max,\alpha}/A_{max,\alpha}$ has been shown to relate to the strain in the polyene chain of the retinal, the value for $[\Theta]_{max,\beta}/A_{max,\alpha}$ relates to the distortion in the β -ionone ring portion of the chromophore (*34*−*36*, *38*). In addition, the maximal ellipticity of the β-band has also been directly related to the absorbance of this band ($[\Theta]_{max,\beta}/A_{max,\beta}$). The differences in these ratios for the two pigments are discussed to be indicative of additional strain in the 10-methyl chromophore.

Photosensitivity of the Analogue Pigment. A comparison of the photosensitivity of 10-methyl rhodopsin, isorhodopsin, and rhodopsin is shown in Figure 4. This figure shows a plot of $-\log[10^{A_t} - 10^{A_f}]$ as a function of time. Both A_t and A_f were determined relative to a baseline set by the 650 nm absorbance in the same spectrum. The ratio of the slopes of these lines yields the photosensitivity of 10-methyl and isorhodopsin relative to rhodopsin. The photosensitivity of the 10-methyl pigment was found to be 49 ± 6% of that of rhodopsin. The reported error is based on two independent experiments on different batches of pigment. Thus, taking the ratio of the molar extinction coefficients at 497 nm (0.60 ± 0.05) into consideration, the quantum yield of the 10-methyl analogue was calculated to be 0.55 ± 0.07. In a similar way the quantum yield of isorhodopsin was determined to be 0.27 ± 0.04, in good agreement with previously published results (*27*, *28*).

MetaI → MetaII Transition. In contrast to rhodopsin, illumination of the 10-methyl analogue pigment at 10 °C

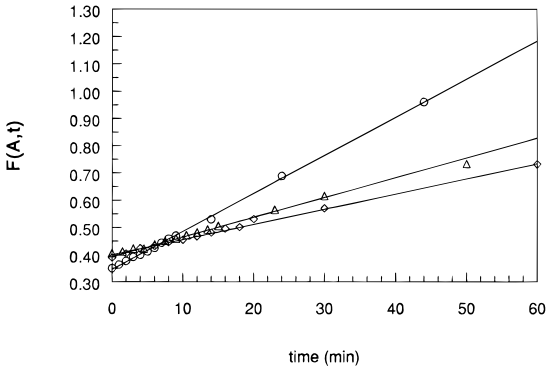

FIGURE 4: The photosensitivity of 10-Me-rhodopsin (△) and isorhodopsin (◇) compared to that of rhodopsin (○). $F(A,t) = -\log[10^{A_t} - 10^{A_f}]$, where A_t denotes the absorbance of the samples at the excitation wavelength (497 nm) as function of illumination time and A_f is the 497 nm absorbance of the fully bleached sample. The initial absorbance at 497 nm was 0.16 ± 0.007 OD/cm for all samples. The ratio of the slope of the lines describing the 10-Me-rhodopsin, isorhodopsin, and rhodopsin data ($r^2 > 0.998$ in all cases) is used to determine the quantum yield of the 10-Me and isorhodopsin pigments, relative to that of rhodopsin (see text).

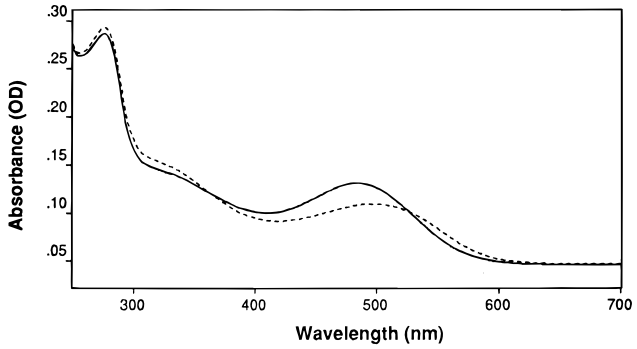

FIGURE 5: Photoproduct (solid line) obtained directly after illumination of a 10-Me-rhodopsin sample (dashed line) at 25 °C. The 10-Me MetaI intermediate (solid line) has its λ_{max} at 490 nm. At this temperature, 10-Me MetaI only slowly decays to 10-Me MetaII (380 nm) ($t_{1/2}$ = 40 min).

only produced a MetaI-like intermediate. This 10-methyl MetaI has its absorbance maximum at 490 nm and thus is blue shifted to a similar extent relative to dark pigment as MetaI (480 nm) from rhodopsin (498 nm). Only at temperatures higher than about 20 °C the 10-methyl MetaI decayed to a photointermediate with absorbance characteristics of MetaII (unprotonated Schiff base, λ_{max} at 380 nm). Figure 5 shows the UV−visible spectrum of 10-Me MetaI obtained at 25 °C. Interestingly, the absorbance of the 10-Me MetaI intermediate at 490 nm is significantly larger than that of 10-Me-rhodopsin at 506 nm, indicating that the extinction of the all-*trans*-10-Me-chromophore is quite similar to that of native MetaI. The decay of the 10-Me MetaI to MetaII intermediate was followed kinetically at various temperatures. An Arrhenius plot of these data (Figure 6) yielded an activation energy E_A of 155 ± 10 kJ/mol for the MetaI to MetaII transition in the 10-methyl pigment, which is similar to that of rhodopsin [156 kJ/mol, (*39*)]. It is very striking that at physiological temperature, where native MetaI decays to MetaII in milliseconds, 10-Me MetaI still has a half-life of several minutes.

FTIR Difference Spectroscopy. Figure 7 shows the infrared difference spectra of the rhodopsin to Batho, MetaI, and MetaII transitions for both rhodopsin and 10-Me-

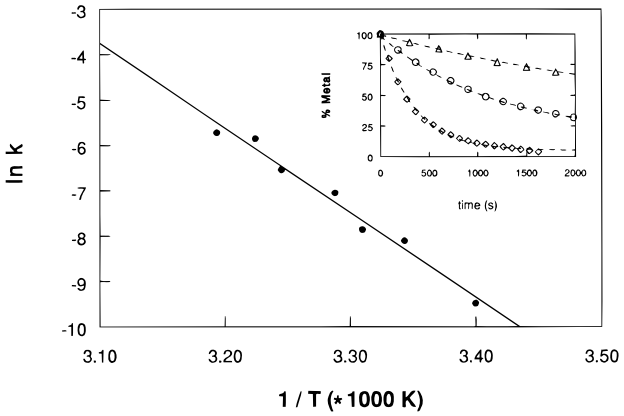

FIGURE 6: Arrhenius plot for the 10-Me MetaI to MetaII transition. An activation energy (E_A) of 155 ± 10 kJ/mol was calculated from these data. Inset shows the decay of 10-Me MetaI to MetaII at 26 (△), 31 (○), and 37 °C (◇). Data points were fitted with monoexponential functions ($r^2 > 0.998$) from which the transition rates (k) were determined.

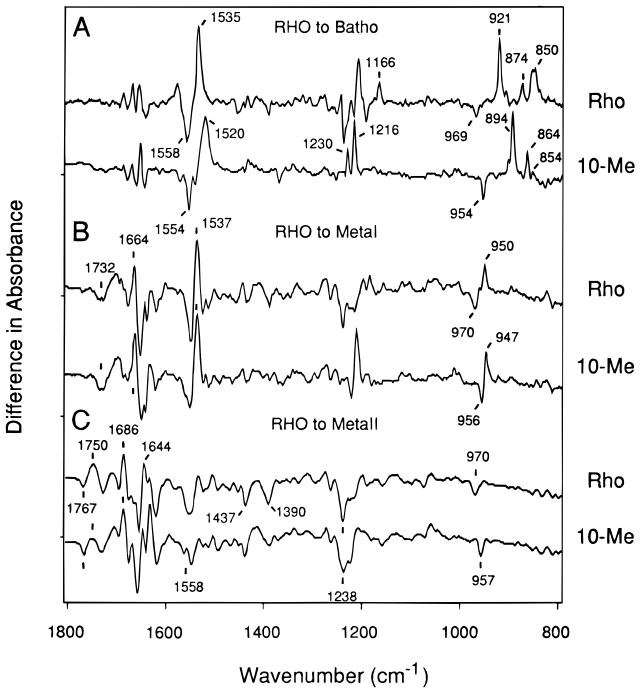

FIGURE 7: FTIR difference spectra of the (A) rhodopsin to Batho (90 K), (B) rhodopsin to MetaI (253 K), and (C) rhodopsin to MetaII transition [taken at 283 and 310 K for rhodopsin (Rho) and 10-Me-rhodopsin (10-Me), respectively].

rhodopsin. In these spectra, rhodopsin bands are negative. It is clear that, going from Batho to MetaII, an increasing number of bands appear in the 1800−1550 cm^{-1} region, indicative of a gradual increase in protein activity (*6*, *7*). The major peaks in the spectral region from 1560 cm^{-1} downward mainly contain information about changes in conformation of the chromophore. Since especially the rhodopsin to Batho difference spectra are dominated by changes in the vibrational state of the retinal chromophore due to isomerization and conformational strain, we expect that this transition will yield the most pronounced differences in the FTIR spectra of the two pigments. This indeed is evident from the spectra presented in Figure 7A.

Most of the bands in the rhodopsin to Batho difference spectrum have been assigned to specific vibrations of the

retinal backbone (C═C and C−C stretch vibrations at ∼1550 and ∼1200 cm^{-1}, respectively) and hydrogen-out-of-plane (HOOP) vibrations, absorbing below 1000 cm^{-1} (*10, 16, 40*). In the 10-Me-rhodopsin to 10-Me Batho difference spectrum, only the small, yet very characteristic, changes in the amide I region (1700−1650 cm^{-1}) are reproduced. These difference bands probably represent subtle conformational changes in the protein moiety. Bands at 1558 cm^{-1} (−) and 1535 cm^{-1} (+) in the rhodopsin spectrum have been assigned to the C_7═C_8 and the C_{11}═C_{12} stretching modes (*10*) and are downshifted in the 10-Me pigment spectrum to 1554 (−) and 1520 (+). The downshift of these bands most likely reflects a more delocalized electronic structure across the retinal polyene chain. More pronounced differences are found in the fingerprint (1350−1150 cm^{-1}) and HOOP (1000−700 cm^{-1}) region. Changes in the fingerprint region [the absence of the 1238 (−), 1192 (−) and 1166 cm^{-1} (+) bands] are probably caused by various contributions, as will be discussed below. The intensity of the bands in the HOOP region indicates that, like the native chromophore, the 10-methyl-chromophore also contains out-of-plane distortions. The 969 cm^{-1} band of rhodopsin has been assigned to the strongly coupled C_{11}H and C_{12}H wags (HC_{11}═C_{12}H A_2 HOOP), indicative of torsion in the C_{10}···C_{13} region (*9, 40*). The positive bands at 921, 875, and 850 cm^{-1} in bathorhodopsin have been shown to contain contributions of the C_{14}H (848 cm^{-1}) and HC_7═C_8H B_g (838) and the (uncoupled) C_{11}H (921) and C_{12}H (858) and C_{10}H (874) wags (*10*). Tentative assignments of the bands in the 10-methyl rhodopsin to Batho difference spectrum will be presented below.

The rhodopsin to MetaI difference spectra (Figure 7B) are highly similar for rhodopsin and 10-methyl rhodopsin, indicating that this transition involves very similar conformational changes in both pigments. In particular, the region between 1800 and 1470 cm^{-1}, which mainly represents structural rearrangements in the protein moiety, is almost identical. Similar to the rhodopsin to Batho transition, the most pronounced differences between the two pigments are found in the fingerprint and HOOP region. Importantly, it is evident from the similarity of these spectra in the HOOP region that, as for native rhodopsin, the 10-Me-chromophore has reached a relaxed all-*trans* conformation at this stage.

The 10-methyl-rhodopsin to MetaII spectrum (Figure 7C) was taken at 37 °C and shows band patterns which are nearly identical with those observed with native MetaII (10 °C), indicating that the "active" 10-Me analogue adopts a conformation very close to native MetaII. Native MetaII decays too rapidly at 37 °C to be reliably measured by FTIR difference spectroscopy. Characteristic MetaII difference bands [1767 (−), 1750 (+), 1710 (+), and 1686 (+) cm^{-1}] are clearly evident in the 10-Me spectra as well.

In view of the very striking effect of the 10-methyl group on the MetaI → MetaII transition, we investigated whether the kinetics of earlier steps in the photocascade also were affected. Indeed we observed a significant change in the temperature dependence of the Batho → Lumi transition. Figure 8 shows the FTIR difference data obtained upon illuminating of 10-methyl rhodopsin at 90, 178, 203, 228, and 253 K. These spectra are scaled with respect to the 954 cm^{-1} (−) band. At 178 K, difference spectra are obtained which are basically identical with those taken at 90 K. At

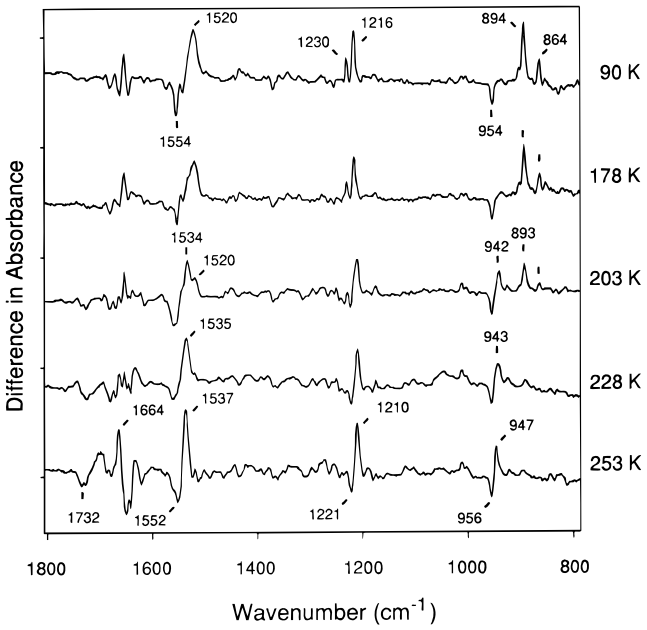

FIGURE 8: FTIR difference spectra obtained upon illuminating 10-Me-rhodopsin at 90, 178, 203, 228, and 253 K, displayed from top to bottom. The Batho-HOOP signals at 894 and 864 cm^{-1} are present even in the spectrum obtained at 203 K; however, at this temperature a slow decay of these bands was observed (see text). The spectra are scaled with respect to the 954 cm^{-1} (−) band of 10-Me-rhodopsin. From 228 K on, the amide and fingerprint regions gradually show more of the MetaI characteristics.

203 K, we observed a slow decay of the 894 (+) HOOP mode in favor of the 942 cm^{-1} (+) band and a concurrent decrease of the 1520 (+) band in favor of the 1534 cm^{-1} (+) band ($t_{1/2} \approx 15$ min, not shown), indicating that 10-Me Batho slowly decays to the next intermediate. It was also observed that with the loss of HOOP signal, photoregeneration after recooling to 90 K became less efficient. Only at 228 K the strong HOOP mode observed at 894 cm^{-1} is completely absent, but, even at this temperature, the characteristic 1655 (−), 1635 (+) cm^{-1} pair of native Lumi is not observed (*7, 41*). Whereas in rhodopsin, the Batho → Lumi transition already occurs at 135 K, and Lumi is characterized by the absence of the strong HOOP modes indicative of a relaxed all-*trans*-chromophore, the Batho intermediate of the 10-methyl pigment, including the strained conformation of retinal, seems to prevail up to unusually high temperature.

Transducin Activation. The fluorescence increase of the α-subunit of transducin upon binding of GTP to the receptor−G protein complex was used to assess whether the 10-methyl pigment could act as a functional photoreceptor (*31, 32*). In Figure 9, the 10-methyl pigment is compared to native rhodopsin and indeed appears to be capable of activating transducin, albeit at an initial rate of about 20% of that of rhodopsin. The ability of the 10-Me pigment to activate transducin agrees with the FTIR difference data, which show that the structural features of 10-Me MetaII are nearly identical with those of native MetaII.

DISCUSSION

Analogue Pigment Formation. The 10-methyl homologue of 11-*cis*-retinal was shown before to form a pigment absorbing at 508 nm (*20*), for which a quantum yield of 0.32

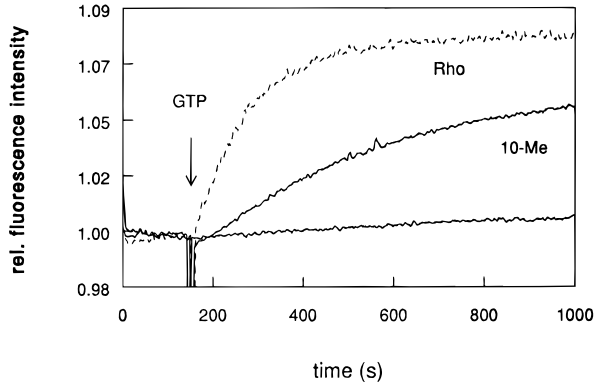

FIGURE 9: Signaling capacity of 10-Me-rhodopsin. The G-protein activation by the 10-Me pigment (solid line) is compared to that of rhodopsin (dashed line), at 20 °C. From the initial slopes of such curves we estimated the activation rate for the 10-Me pigment at 20 °C to be about 20% of that of rhodopsin. Concentrations of pigment and transducin were 5 and 100 nM, respectively. At the time point indicated by the arrow, GTP-γ-S was added to 2.5 μM. Bottom trace shows control with no pigment added.

$\pm$ 0.06 was reported (*27*). In our hands, 10-methyl-11-*cis*-retinal yields a pigment with a λ_{max} of 506 $\pm$ 2 nm, and a quantum yield of 0.55 $\pm$ 0.07. While the difference in λ_{max} is within experimental error, the reported values of the quantum yield deviate to a significant extent. The discrepancy between the reported quantum yields appears to be largely caused by the different values used for the extinction coefficient of the 10-methyl pigment. Liu et al. (*27*) based their calculations on the extinction coefficient determined for the 10-fluoro analogue of rhodopsin, which was reported to be 0.75 of that of rhodopsin (*20*). A separate value for the 10-Me analogue was not reported. Our data show that the extinction coefficient of the 10-methyl pigment (0.60 of that of rhodopsin) is significantly lower. Taking our value would increase the quantum yield reported by Liu et al. to 0.40 $\pm$ 0.08, which agrees within experimental error with our data. Interestingly, the reduction of the quantum yield of photoisomerization of the native pigment due to the addition of a methyl group at the C_{10} position of the chromophore (0.67 $\rightarrow$ 0.55) is also exhibited by the 13-demethyl pigment (0.47 $\rightarrow$ 0.35) (*28*). However, it should be noted that deviating values for the quantum yield of the 13-demethyl pigment have been reported by Gärtner and coworkers (*42, 43*).

Spectral Properties and Chromophore Conformation of 10-Me-Rhodopsin. Both the observed red shift of the λ_{max} in the UV−visible spectrum of the analogue pigment and the downshifted ethylenic stretching modes in the 10-Me-rhodopsin to Batho FTIR difference spectrum are indicative of a more delocalized charge distribution in the conjugated retinal moiety (*44*). These effects may relate to the electrodonating properties of the methyl group. However, the λ_{max} of the protonated Schiff base of all-*trans*-10-methyl-retinal (imine formed by reaction of all-*trans*-10-methyl-retinal and a 30-fold molar excess of decylamine in hexane, protonated form studied in 1% Ammonyx-LO at pH 2) was observed at 438 $\pm$ 1 nm, only slightly red shifted from that of all-*trans*-retinal (436 $\pm$ 1 nm, P. Bovee and F. DeLange, unpublished material). Thus, the 8 nm red shift of the absorbance maximum of 10-Me-rhodopsin is more likely caused by an altered conformation and/or positioning of the 10-Me-chromophore in the binding pocket of opsin, relative to that of 11-*cis*-retinal.

All available evidence indicate that the 10-Me-chromophore conformation is more perturbed than that in rhodopsin. First, the slow pigment formation suggests suboptimal accessibility of the retinal homologue into the binding pocket of opsin. Second, the 10-methyl group seems to impose an enhanced torsional strain in the chromophore, which is apparent from the stronger β-band in the UV−visible spectrum of the 10-Me pigment, from the CD spectra, as well as from the increased intensity of the (rhodopsin) HOOP band in the infrared difference spectrum of the 10-Me-rhodopsin to Batho transition.

The β-band in CD spectra of visual pigments has been shown to be sensitive to distortions in the ionone ring portion of the retinal. Recently, Wada et al. reported that the planarization of the $C_5-C_6-C_7-C_8$ torsion angle in 11-*cis*-8,18-methanoretinal doubles the value of $[\Theta]_{max,\beta}/A_{max,\alpha}$ (*38*). However, the reduced molar extinction of the α-band in the UV−visible spectrum of the 10-Me pigment makes a comparison of the $[\Theta]_{max,\beta}/A_{max,\alpha}$ parameter between native and 10-Me-rhodopsin less useful. By relating the maximal ellipticity of the β-band directly to the absorbance of the same band, we observed an almost 50% decrease of the $[\Theta]_{max,\beta}/A_{max,\beta}$ parameter for 10-Me-rhodopsin, which may well reflect increased torsion in the C_6-C_7 bond. From the increased $[\Theta]_{max,\alpha}/A_{max,\alpha}$ value for 10-methyl rhodopsin and the increase in intensity of the rhodopsin HOOP vibration at 954 cm^{-1} relative to the 969 cm^{-1} band in the native rhodopsin to Batho spectrum (assignments discussed below), we infer that the polyene chain of the chromophore in the analogue pigment is in a more strained conformation than 11-*cis*-retinal in native rhodopsin (*28, 34, 35, 40*). Indeed, recent solid-state ^{13}C NMR analyses of 10-methyl-rhodopsin also indicate increased torsional strain in the $C_{10}\cdots C_{13}$ region (Verdegem et al., in preparation).

Photoactivation of the Receptor. The amide and carboxyl region (1800−1400 cm^{-1}) in the FTIR difference spectrum of the 10-Me-rhodopsin to MetaII transition, measured at 37 °C, differs only very slightly from that of rhodopsin at 10 °C. In fact, the subtle differences in these spectral regions may well be attributed to temperature effects. All available evidence indicates that the accompanying conformational changes in the 10-methyl pigment are identical with those in rhodopsin. Our observation that the analogue pigment is able to activate transducin corroborates this conclusion. The lower absolute rate of activation by the 10-methyl pigment is attributed to the relatively slow formation of 10-Me MetaII under the experimental conditions, which now has become the rate-limiting step. Notably, although the reaction rates of the MetaI to MetaII transition are quite different in the 10-methyl pigment, the Arrhenius activation energy for this transition is surprisingly similar to that determined for native rhodopsin. This further supports our conclusion, that similar protein conformational changes are involved. Moreover, the effect of the additional methyl group on the thermal activation of the MetaI to MetaII transition appears to be predominantly entropy related. A similar observation was reported for the effect of detergent solubilization on the reaction rate of the MetaI to MetaII transition in native rhodopsin (*39*).

Ligand−Receptor Interactions; FTIR Analysis of the 10-Me-Rhodopsin Photocascade. Our data show that the 10-methyl group, apart from the structural effects it imposes on the dark state conformation of the chromophore, also has a striking effect upon the photocascade up to at least MetaII. Although the 10-Me-rhodopsin to Batho difference spectrum differs strongly from that of rhodopsin, some of the differences in the ethylenic and fingerprint regions can be explained by the mere presence of the additional methyl group and do not necessarily point at altered ligand−protein interactions. In contrast to the ethylenic stretch modes, the vibrational frequency of the fingerprint modes are shifted upward at increasing charge delocalization of the retinal. Moreover, the 10-Me group is likely to affect the coupling between the fingerprint modes. The coupling of the C_{10}−C_{11} polyene single bond stretch and the C_{10}−Me stretch, for example, is expected to result in an upshift of the band by ∼100 cm^{-1} (*28*) and may explain the absence of the native positive 1166 cm^{-1} band in the analogue spectrum. Further, the loss of coupling with the 10-H (by deuteration) can upshift the C_8−C_9 band as much as 80 cm^{-1} (*16*). Moreover, also in the 10-D pigment, the C_{14}−C_{15} band of rhodopsin (1192 cm^{-1}) was not observed, while that of Batho was shifted to 1220 cm^{-1}. Thus, we tentatively assign the 1216 cm^{-1} (+) band to the C_{14}−C_{15} stretch in 10-Me-Batho. The absence of the 1238 cm^{-1} (−) band, assigned to the C_{12}−C_{13} vibration in rhodopsin (*16*), is also consistent with RR data on the 10-D pigment: the C_{12}−C_{13} stretch vibrations of 10-D-rhodopsin and Batho were shown to practically coincide at 1235 cm^{-1}. Therefore, we assign the 1230 cm^{-1} (+) band to the partially canceled C_{12}−C_{13} stretching vibration of 10-Me Batho.

The strong HOOP vibrations observed in the 10-Me-rhodopsin to Batho FTIR difference spectrum indicate that there are out-of-plane distortions of the chromophore as there are in native rhodopsin. By analogy, we tentatively assign the 954 cm^{-1} negative band to the HC_{11}═$C_{12}H$ A_2 HOOP modes of 10-Me-rhodopsin, again, in agreement with RR data on 10-D-rhodopsin (*9*). In fact, the 954 cm^{-1} band of 10-Me-rhodopsin band is more intense than the 969 cm^{-1} observed in native rhodopsin, consistent with a more strained conformation of the polyene chain of the 10-Me-chromophore as discussed above. We further assign the 10-Me-Batho band at 894 cm^{-1} to the $C_{11}H$ wag. In native rhodopsin, this mode absorbs at 921 cm^{-1}, a frequency characteristic for an isolated wag. The observed downshift of this band, not observed in the 10-D-Batho RR data, may be caused by a net displacement of the 10-methyl-chromophore, such, that the C_{11} gets in closer vicinity of a negatively charged protein residue. In native rhodopsin, the C_{12} was tentatively placed near a negatively charged residue to explain the uncoupling of the $C_{11}H$ and $C_{12}H$ wags upon photoisomerization and the 60 cm^{-1} downshift of the latter (*8*, *9*). On the basis of the 10-D-Batho RR data, it is tempting to assign the 864 and 854 cm^{-1} bands to the HC_7═C_8H B_g and $C_{14}H$ HOOPS, respectively (*10*). We note that these assignments are preliminary and await direct proof from labeling studies which currently are in progress. If the assignment of the 864 cm^{-1} band proves to be correct, the strength of this band relative to the 862 cm^{-1} band in 10-D-Batho would indicate enhanced torsional strain in the C_7═C_8 bond in 10-Me-Batho.

According to our present evidence, apart from the lowered quantum yield of isomerization, the 10-methyl group does not seem to interfere structurally with the photocascade up to formation of a Batho intermediate with a strained all-*trans*-chromophore. Importantly, the fingerprint region in our FTIR difference spectra of the 10-Me-rhodopsin to Batho transition shows good correspondence with the RR data on 10-D-labeled rhodopsin and bathorhodopsin (*16*). We conclude that the primary photoreaction in the analogue pigment indeed is an 11-*cis* to all-*trans* photoisomerization. The observation that 10-Me-bathorhodopsin can be photoreversed without significant loss of signal or spectral shifts supports this conclusion.

In contrast to what is found for native rhodopsin, the 10-Me-HOOP signals were detectable up to 210 K, indicating that steric interactions between the 10-Me-retinal and opsin hamper the relaxation of strain in the retinal moiety. Likewise, the slow formation of 10-Me-MetaII is attributed to steric interactions with another protein residue. Several bands in the infrared difference spectra hint at the involvement of protein residues, however, the exact interaction sites in the protein cannot yet be identified. For example, the 10-Me-rhodopsin to MetaI and MetaII difference spectra show a shoulder at 1558 cm^{-1} and a significant loss of intensity of the 1644 cm^{-1} (+) band. Moreover, in the 10-Me-rhodopsin to MetaII spectra, the (native) 1655 cm^{-1} (−) band is reproducibly observed at 1659 cm^{-1}, possibly due to the absence of a shoulder at 1663 cm^{-1} in the native spectrum. We note, however, that an incomplete MetaI to MetaII transition and the different experimental temperatures may induce small differences in the amide regions. Isotopic labeling should elucidate the nature of the ligand−protein interactions throughout the photocascade of the 10-methyl pigment.

Relation to Other (De)Methyl Rhodopsin Analogues. Together with previous studies on rhodopsins containing a demethyl-11-*cis*-retinal analogue, this work provides a consistent picture on the conformational freedom of the retinal in the binding pocket of opsin as well as on the mechanism of energy storage in the Batho intermediate of rhodopsin. In short, the 9-demethyl compound was reported to have a fully disturbed photocascade, in which a clear Batho intermediate could not be detected at 80 K (see, e.g., ref 45). Furthermore, the 9-demethyl-MetaII-like intermediate was found to have a protonated Schiff base, unusual structural features in the corresponding FTIR difference spectrum, and was incapable of activating transducin. The 13-demethyl rhodopsin analogue exhibits a basically normal photocascade (see, e.g., ref 46) and G-protein activity, and, interestingly, was also found to activate transducin in the dark (*47*). While the 13-methyl group seems to be of prime importance in suppressing dark activity of the receptor, the 9-methyl group seems to be an important factor for the correct positioning of the retinal in the binding pocket of opsin. Moreover, the 9-methyl group seems to provide the necessary fixation of parts of the chromophore, which, upon photoisomerization, gives rise to the torsional strain in the chromophore. Our results clearly show, that addition of a methyl group at the 10 position results in a completely different phenotype. Not unexpectedly, the 10-methyl pigment behaves as a functional photoreceptor, including activation of the G-protein transducin. However, the ad-

ditional methyl group severely perturbs the kinetics of the photocascade at two stages (Batho → Lumi and MetaI → MetaII), without significant effects on the conformational changes in the various transitions. The most logical explanation is that sterical interaction of the 10-methyl group with the protein environment changes the free energy barriers of these two transitions and forces the system through a slightly different trajectory. In the Batho → Lumi transition it probably is the relaxation of strain in the chromophore which now becomes rate limiting, and is obstructed by protein residues. In the MetaI → MetaII transition, the chromophore is fully relaxed and the 10-methyl group probably obstructs conformational changes in the protein, involving adjacent residues. It follows that, most likely, different protein residues are involved in the interaction with the 10-methyl group during these transitions. The available 3-D structure has not enough resolution to allow selection of potential candidates for these residues, but we are currently trying to identify these by scanning mutagenesis.

The current picture is that the photon energy is stored as torsional strain in the chromophore at the Batho stage (*10*, *48*) and that the energy released upon relaxation of the strain is used to drive the protein conformational changes in the photocascade dark reaction. This is consistent with our observation that as long as the HOOP signals prevail, only very small changes in the Amide I and Amide II region are observed in the FTIR difference spectra of the 10-methyl pigment.

Conclusion. The salient result of this study is that the addition of a methyl group at position 10 of the chromophore strongly perturbs two stages of the photocascade. Interestingly, although the additional methyl group somewhat reduces the efficiency of the process, photoisomerization of this chromophore results in a "normal" Batho intermediate with a strained all-*trans*-chromophore conformation. However, then, it first markedly retards relaxation of the photoisomerized chromophore and the occurrence of structural changes in the protein moiety. The important conclusion is that relaxation of the chromophore drives the subsequent structural changes in the receptor. Subsequently, it severely interferes with the conformational transition of the MetaI intermediate into the "active" intermediate, MetaII. Clearly, the chromophore has not much conformational freedom and the interaction between ligand and protein has become very finely tuned in order to allow highly efficient photon capture as well as very selective triggering of conformational changes in the protein moiety toward receptor activation.

ACKNOWLEDGMENT

We thank Dr. R. Mathies for stimulating discussions and Ir. C. Houbiers for expert assistence with the CD experiments.

REFERENCES

1. Emeis, D., Kühn, H., Reichert, J., and Hofmann, K. P. (1982) *FEBS Lett. 143*, 29−34.
2. Kibelbek, J., Mitchell, D. C., Beach, J. M., and Litman, B. J. (1991) *Biochemistry 30*, 6761−6768.
3. Rath, P., DeCaluwé, G. L. J., Bovee-Geurts, P. H. M, DeGrip, W. J., and Rothschild K. J. (1993) *Biochemistry 32*, 10277−10282.
4. Fahmy, K., Jäger, F., Beck, M., Zvyaga, T. A., Sakmar, T. P., and Siebert, F. (1993) *Proc. Natl. Acad. Sci. U.S.A. 90*, 10206−10210.
5. DeCaluwé, G. L. J., Bovee-Geurts, P. H. M., Rath, P., Rothschild, K. J., and DeGrip, W. J. (1995) *Biophys. Chem. 56*, 79−87.
6. Rothschild, K. J., Cantore, W. A., and Marrero, H. (1983) *Science 219*, 1333−1335.
7. DeGrip W. J., Gray, D., Gillespie, J., Bovee, P. H., Van den Berg E. M., Lugtenburg J., and Rothschild, K. J. (1988) *Photochem. Photobiol. 48*, 497−504.
8. Eyring, G., Curry, B., Mathies, R., Fransen, R., Palings, I., and Lugtenburg, J. (1980) *Biochemistry 19*, 2410−2418.
9. Eyring, G., Curry, B., Broek, A, Lugtenburg, J., and Mathies, R. (1982) *Biochemistry 21*, 384−393.
10. Palings, I., van den Berg, E. M. M., Lugtenburg, J., and Mathies, R. A. (1989) *Biochemistry 28*, 1498−1507.
11. Honig, B., Dinur, U., Nakanishi, K., Balogh-Nair, V., Gawinowicz, M. A., Arnaboldi, M., and Motto, M. G. (1979) *J. Am. Chem. Soc. 101*, 7084−7086.
12. Warshel, A., and Barboy, N. (1982) *J. Am. Chem. Soc. 104*, 1469−1676.
13. Birge, R. R., Einterz C. M., Knapp., H. M., and Murray L. P. (1988) *Biophys. J. 53*, 367−385.
14. Buda, F., DeGroot, H. J. M., and Bifone, A. (1996) *Phys. Rev. Lett. 77*, 4474−4477.
15. Vos, F. L. J., Aalberts, D. P., and van Saarloos W. (1996) *Phys. Rev. B 53*, 14922−14928.
16. Palings, I., Pardoen, J. A., van den Berg, E. M. M., Winkel, C., Lugtenburg, J., and Mathies, R. A. (1987) *Biochemistry 26*, 2544−2556.
17. Smith, S. O., Courtin, J., de Groot, H., Gebhard, R., and Lugtenburg, J. (1991) *Biochemistry 30*, 7409−7415.
18. Corson, D. W., and Crouch, R. K. (1996) *Photochem. Photobiol. 63*, 595−600.
19. DeGrip, W. J., DeLange, F., Bovee, P., Verdegem, P. J. E., and Lugtenburg, J. (1997) *Pure Appl. Chem. 69*, 2091−2098.
20. Asato, A. E., Denny, M., Matsumoto, H., Mirzadegan, T., Ripka, W. C., Crescitelli, F., and Liu, R. S. H. (1986) *Biochemistry 25*, 7021−7026.
21. DeGrip, W. J., VanOostrum, J., Bovee-Geurts, P. H. M., VanderSteen, R., VanAmsterdam, L. J. P., Groesbeek, M., and Lugtenburg, J. (1990) *Eur. J. Biochem. 191*, 211−220.
22. Groenendijk, G. W. T., DeGrip, W. J., and Daemen, F. J. M. (1980) *Biochim. Biophys. Acta 617*, 430−438.
23. Hendriks, T., Klompmakers, A. A., Daemen, F. J. M., and Bonting, S. L. (1976) *Biochim. Biophys. Acta 433*, 271−281.
24. DeGrip, W. J., Olive, J., and Bovee-Geurts, P. H. M. (1983) *Biochim. Biophys. Acta 734*, 168−179.
25. DeLange, F., Merkx, M., Bovee-Geurts, P. H. M., Pistorius, A. M. A., and DeGrip, W. J. (1997) *Eur. J. Biochem. 243*, 174−180.
26. Dartnall, H. J. A. (1972) in *Handbook of Sensory Physiology* (Dartnall, H. J., Ed.) Vol. 7, Part 1, pp 122−145, Springer Berlin.
27. Liu, R. S. H., Crescitelli, F., Denny, M., Matsumoto, H., and Asato, A. E. (1986) *Biochemistry 25*, 7026−7030.
28. Kochendoerfer, G. G., Verdegem, P. J. E., van der Hoef, I., Lugtenburg, J., and Mathies, R. A. (1996) *Biochemistry 35*, 16230−16240.
29. Hubbard, R., and Wald, G. (1952) *J. Gen. Physiol. 36*, 269−315.
30. Clark, N. A., Rothschild, K. J., Luippold, D., and Simon, B. (1980) *Biophys. J. 31*, 65−96.
31. Phillips, W. J., and Cerione, R. A. (1988) *J. Biol. Chem. 30*, 15498−15505.
32. Fahmy, K., and Sakmar, T. P. (1993) *Biochemistry 32*, 7229−7236.
33. Kühn, H. (1984) *Prog. Retinal Res. 3*, 123−156.
34. Kropf, A., Whittenberger, B. P., Goff, S. P., and Waggoner, A. S. (1973) *Exp. Eye Res. 17*, 591−606.
35. Rafferty, C. N., Cassim, J. Y., and McConnell, D. G. (1977) *Biophys. Struct. Mech. 2*, 277−320.

36. Horiuchi, S., Tokunaga, F., and Yoshizawa, T. (1980) *Biochim. Biophys. Acta 591*, 445−457.
37. Okada, T., Matsuda, T., Kandori, H., Fukada, Y., Yoshizawa, T., and Shichida, Y. (1994) *Biochemistry 33*, 4940−4946.
38. Wada, A., Tsutsumi, M., Inatomi, Y., Imai, H., Shichida, Y., and Ito, M. (1995) *Chem. Pharm. Bull. 43*, 1419−1421.
39. Arnis, S., and Hofmann, K. P. (1993) *Proc. Natl. Acad. Sci. U.S.A. 90*, 7849−7853.
40. Mathies, R. A., Smith, S. O., and Palings, I. (1987) in *Biological Applications of Raman Spectrometry* (Spiro, T. G., Ed.) Vol. 2, pp 59−108, John Wiley & Sons.
41. Ganter, U. M., Gärtner, W., and Siebert, F. (1988) *Biochemistry 27*, 7480−7488.
42. Gärtner, W., and Ternieden, S. (1996) *J. Photochem. Photobiol., B. 33*, 83−86.
43. Koch, D., and Gärtner, W. (1997) *Photochem. Photobiol. 65*, 181−186.
44. Doukas, A. G., Aton, B., Callender, R. H., and Ebrey, T. G. (1978) *Biochemistry 17*, 2430−2435.
45. Ganter, U. M., Schmid, E. D., Perez-Sala, D., Rando, R. R., and Siebert, F. (1989) *Biochemistry 28*, 5954−5962.
46. Ganter, U. M., Gärtner, W., and Siebert, F. (1990) *Eur. Biophys. J. 18*, 295−299.
47. Ebrey, T. G., Tsuda, M., Sassenrath, G., West, J. L., and Waddell, W. H. (1980) *FEBS Lett. 116*, 217−219.
48. Bifone, A., DeGroot, H. J. M., and Buda, F. (1997) *J. Phys. Chem. B 101*, 2954−2958.

BI972397Y